Crystalline phases of thiourea. I. Model of incommensurate phases

K. Parlinski* and K. H. Michel
Departement Natuurkunde, Universiteit Antwerpen (UIA), B-2610 Wilrijk, Belgium
(Received 25 April 1983; revised manuscript received 1 August 1983)

A one-dimensional model describing the successive phases in completely deuterated thiourea [$SC(ND_2)_2$] is proposed. The stable phases of the model are investigated by numerical and analytical methods. Lock-in phases with wave-vector modulations $\frac{1}{7}$, $\frac{1}{8}$, and $\frac{1}{9}$ have been found. The essential couplings between harmonics of different symmetries have been established.

I. INTRODUCTION

The crystal of deuterated thiourea $SC(ND_2)_2$ undergoes several phase transitions. The highest temperature phase has D_{2h}^{16} (*Pnma*) symmetry[1] and is paraelectric whereas the lowest phase has symmetry C_{2v}^{2} ($Pmc2_1$) and is ferroelectric.[2,1] In addition there exists an intermediate incommensurate phase[3] characterized by an incommensurate wave vector k_m, which in the whole temperature range and under normal pressure changes[4] approximately from the values $\frac{1}{7}$ to $\frac{1}{9}$. Close to the ferroelectric phase, the incommensurate phase is locked[5] to the commensurate phase $\frac{1}{9}$. The commensurate phase $\frac{1}{7}$ appears at higher pressures.[6] The phase diagram for deuterated thiourea is shown in Fig. 1. Although the wave vector passes the value $\frac{1}{8}$, no trace of such a lock-in phase has been noticed in neutron scattering experiments at zero electric field. The phase transition from the incommensurate phase to the $\frac{1}{9}$ lock-in phase shows hysteresis.[5] The above-described behavior is in agreement with heat-capacity measurement,[7] elastic constant data obtained by Brillouin scattering technique,[8] and thermal expansion.[9] The measurements made on nondeuterated crystals $SC(NH_2)_2$ exhibit a nonzero value of spontaneous polarization inside the region of the incommensurate phase.[10,11]

The orthorhombic unit cell in the high-temperature phase of thiourea is shown in Fig. 2. It contains four molecules. The $SC(ND_2)_2$ molecule is almost flat[12] and then its symmetry is C_{2v}. The twofold-symmetry axis of the molecule and one of its symmetry planes are parallel to the (a,c) plane of the unit cell. Proceeding along the b axis, one notices the planes with alternating molecular orientations. Their projections onto the plane (a,c) are shown in Fig. 3.

The ferroelectric phase has a unit cell of approximately the same size as the high-temperature phase and it arises as an effect of a condensation of B_{3u} mode at $k=0$. The ferroelectric polarization results from the rotations of each molecule around the b axis[1] by an angle φ of about 5.1°. The rotational displacements in two neighboring (a,c) planes are opposite, as is indicated in Fig. 3.

The modulation in the incommensurate phase of thiourea propagates along the b direction.[4,13,14] It can be visualized as a sequence of (a,c) planes characterized by a changeable value of the molecular orientation φ.

The incommensurate phase is characterized by the presence of satellite reflections in the x-ray diffraction pattern. The intensity of the first-order satellite increases with decreasing temperature. The same behavior has been observed[15] for the second-order satellite.

The inelastic coherent neutron scattering experiments have revealed, in addition to critical scattering,[16] the ex-

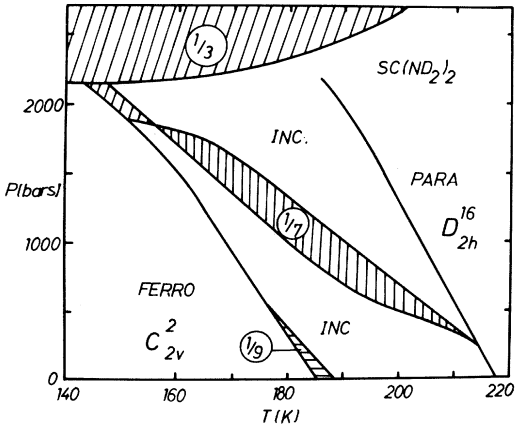

FIG. 1. Temperature-pressure phase diagram (Ref. 6). Regions $\frac{1}{3}$, $\frac{1}{7}$, and $\frac{1}{9}$ correspond to the commensurate phases.

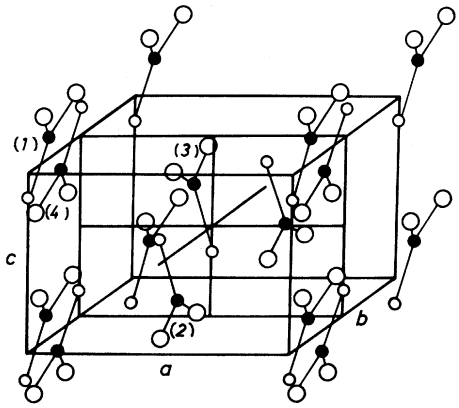

FIG. 2. High-temperature unit cell of thiourea. Molecules 1,2 and 3,4 are in the first and second (a,c) plane, respectively. The ND_2 groups are shown as the larger open circles.

 ©1984 The American Physical Society

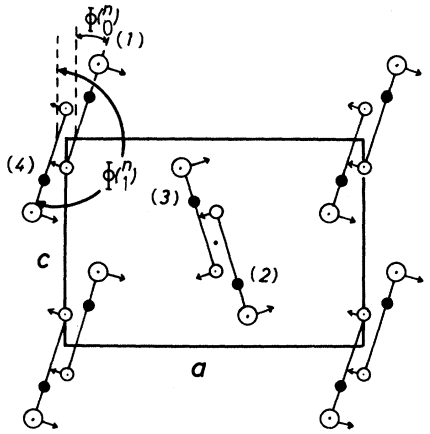

FIG. 3. Projection of the high-symmetry unit cell on the (a,c) plane. Molecules 1,4 and 2,3 are parallel, respectively. The arrows are the librational polarization vectors belonging to the B_{3u} mode.

istence of a soft optic phonon branch[15] in direction b and close to the Brillouin-zone center. This phonon branch has a symmetry $\hat{\tau}_4$ and belongs to the irreducible star k_7 in Kovalev's notation.[17] It shows a pronounced minimum near $k=0.16$. This minimum lowers with decreasing temperature, eventually producing the incommensurate phase. There also exists a transverse acoustic phonon of the same symmetry $\hat{\tau}_4$. The soft optic mode and the transverse acoustic mode couple together giving rise to the static rotational and translational displacements of the thiourea molecules.

Thiourea is sometimes referred to as an experimental model system, where some features that follow from rather general theories[18,19] are realized. On the other hand, one has the proposed continuous models, which are based on a Landau-Ginsburg type of free energy, to describe some properties of the incommensurate phase transitions in thiourea.[20–23] To our knowledge, it has not been possible so far to give a description which accounts in a unified way for the complex set of phases in thiourea, even at atmospheric pressure. It is our purpose in the present paper to undertake such a study. The outline of the paper is as follows.

In Sec. II we propose a discrete one-dimensional model and write the corresponding free energy in terms of orientational displacements of thiourea molecules in successive (a,c) planes perpendicular to the crystallographic b axis. Harmonic and anharmonic terms contribute to the local and to the intermolecular potential. Force constants up to nine neighbors must be taken into account. An approximate analytical solution of the model in terms of a single cosine modulation of $\hat{\tau}_4$ symmetry is derived in Sec. III. In Secs. IV and V we present a numerical solution of the model. The method consists of finding the most stable configuration of a linear chain of 1008 molecules that interact according to the force laws of our model. The numerical results are studied as a function of temperature and of certain other parameters of the model, in particular the strength of the local potential. In addition to modulated incommensurate phases, commensurate lock-in phases $\frac{1}{8}$, $\frac{1}{7}$, and $\frac{1}{9}$ are obtained. Squaring effects in the incommensurate state and phase dependence in the lock-in states are investigated. Next (Sec. VI) we give an analytic description of the free energy in terms of normal modes of $\hat{\tau}_1$ and $\hat{\tau}_4$ symmetry and their corresponding higher harmonics. Stability conditions which lead to relations between various harmonics are discussed and compared with experiment (Sec. VII) and with the numerical results of Sec. V. Our overall conclusion is that the present model accounts qualitatively of the complex situation of the phase diagram in thiourea at atmospheric pressure.

II. ONE-DIMENSIONAL MODEL

From symmetry it follows that the essential features of thiourea can be described within a one-dimensional model. Indeed the structural changes at all phase transitions are related to the soft mode of symmetry $\hat{\tau}_4$ close to $k=0$. That symmetry implies that the orientations of molecules labeled 3 and 2 in Fig. 3 follow from the orientation of molecules 1 and 4, respectively. In other words, the orientational coordinate of one molecule in an (a,c) plane defines the orientation of all other molecules in that plane. Therefore the orientational configuration of one chain of molecules along the b direction is sufficient to represent the paraelectric, ferroelectric, and incommensurate phases.

Taking into account that two successive molecules separated by a distance $b_0/2$ along the chain have alternating orientations and different projections in the (a,c) plane, we see that there are two molecules (for example, 1 and 4 in Fig. 3) per unit cell. The rotation of each molecule is accompanied by a translational shift in the (a,c) plane. Therefore both types of displacements can be described by one coordinate $\varphi(\begin{smallmatrix}m\\ \kappa\end{smallmatrix})$. Here $m=1,2,\ldots,N$ labels the unit cells along the chain and $\kappa=0,1$ denotes the first and the second molecule in the unit cell. Although $\varphi(\begin{smallmatrix}m\\ \kappa\end{smallmatrix})$ is a mixed coordinate caused by translation-rotation coupling,[4] we shall from here on always speak loosely of $\varphi(\begin{smallmatrix}m\\ \kappa\end{smallmatrix})$ as the angle of rotation. Then the coordinate $\varphi(\begin{smallmatrix}m\\ \kappa\end{smallmatrix})$ can be written as

$$\varphi\left(\begin{smallmatrix}m\\ \kappa\end{smallmatrix}\right)=\Phi\left(\begin{smallmatrix}m\\ \kappa\end{smallmatrix}\right)-\Phi_\kappa\,, \tag{2.1}$$

where Φ_κ is the equilibrium thermal average of $\varphi(\begin{smallmatrix}m\\ \kappa\end{smallmatrix})$ in the high-symmetry phase for the sublattice κ and hence $\Phi_1=\Phi_0+\pi$.

Since the unit cell of the one-dimensional model contains two molecules, there are two normal modes present for a given wave vector k. The first one, of $\hat{\tau}_4$ symmetry, corresponds to a rotation of two successive molecules in opposite directions; the second one, of $\hat{\tau}_1$ symmetry, corresponds to a rotation in the same direction. For our one-dimensional model we keep the notations of the corresponding representations of the three-dimensional crystal. Calling η_4 and η_1 the amplitudes of these modes, respectively, we can write a representation of a modulation with a single wave vector k in the form

$$\begin{aligned}\varphi\left(\begin{smallmatrix}m\\ \kappa\end{smallmatrix}\right)=&(-1)^\kappa\eta_4(k)\cos[2\pi k(mb_0+r_\kappa)-\epsilon_4]\\&+\eta_1(k)\cos[2\pi k(mb_0+r_\kappa)-\epsilon_1]\,.\end{aligned} \tag{2.2}$$

Here $r_\kappa=0$ or $b_0/2$ or $\kappa=0$ or 1, respectively, and ϵ_4 and ϵ_1 are phase shifts. The factor $(-1)^\kappa$ ensures that the rotation angle in successive planes alternates its sign in agreement with the polarization vector of the B_{3u} mode.[4,15]

We assume that the free energy of the one-dimensional model per molecule can be written as

$$F=\frac{1}{2N}\sum_{m=1}^{N}\sum_{\kappa=0}^{1}V(\varphi(\begin{smallmatrix}m\\ \kappa\end{smallmatrix})) + \frac{1}{2N}\sum_{m,n=1}^{N}\sum_{\kappa,\mu=0}^{1}W(\varphi(\begin{smallmatrix}m\\ \kappa\end{smallmatrix})-\varphi(\begin{smallmatrix}n\\ \mu\end{smallmatrix})) , \tag{2.3}$$

where we choose

$$V(\varphi(\begin{smallmatrix}m\\ \kappa\end{smallmatrix}))=a\varphi^2(\begin{smallmatrix}m\\ \kappa\end{smallmatrix})+h\varphi^3(\begin{smallmatrix}m\\ \kappa\end{smallmatrix})+b\varphi^4(\begin{smallmatrix}m\\ \kappa\end{smallmatrix}) , \tag{2.4}$$

$$W(\varphi(\begin{smallmatrix}m\\ \kappa\end{smallmatrix})-\varphi(\begin{smallmatrix}n\\ \mu\end{smallmatrix}))=\Phi^{(2)}(\begin{smallmatrix}mn\\ \kappa\mu\end{smallmatrix})[\varphi(\begin{smallmatrix}m\\ \kappa\end{smallmatrix})-\varphi(\begin{smallmatrix}n\\ \mu\end{smallmatrix})]^2 + \Phi^{(4)}(\begin{smallmatrix}mn\\ \kappa\mu\end{smallmatrix})[\varphi(\begin{smallmatrix}m\\ \kappa\end{smallmatrix})-\varphi(\begin{smallmatrix}n\\ \mu\end{smallmatrix})]^4 , \tag{2.5}$$

and where N denotes the total number of unit cells in the linear chain.

We shall also use the following notation of the self-force constants:

$$a=\Phi^{(2)}(\begin{smallmatrix}mm\\ \kappa\kappa\end{smallmatrix}),\quad b=\Phi^4(\begin{smallmatrix}mm\\ \kappa\kappa\end{smallmatrix}) , \tag{2.6}$$

and the force constants to the pth neighbors

$$\alpha_p=\Phi^{(2)}(\begin{smallmatrix}mn\\ \kappa\mu\end{smallmatrix}),\quad \beta_p=\Phi^{(4)}(\begin{smallmatrix}mn\\ \kappa\mu\end{smallmatrix}) , \tag{2.7}$$

where $p=2(n-m)+\mu-\kappa$, since now we measure intermolecular distances in units $b_0/2$. Owing to the existence of the symmetry plane perpendicular to the b direction, the force constants are symmetric, $\alpha_p=\alpha_{-p}$ and $\beta_p=\beta_{-p}$. The functions $V(\varphi(\begin{smallmatrix}m\\ \kappa\end{smallmatrix}))$ and $W(\varphi(\begin{smallmatrix}m\\ \kappa\end{smallmatrix})-\varphi(\begin{smallmatrix}n\\ \mu\end{smallmatrix}))$ represent the local and intermolecular potentials, respectively.

It should be emphasized that expression [(2.3)–(2.5)] of the free energy for the one-dimensional model is an effective free energy. It is thought to be obtained from the Hamiltonian of a three-dimensional crystal after averaging out all nonrelevant degrees of freedom and retaining only those coordinates which refer to the orientational positions along one chain. As a result of this procedure, expressions (2.3)–(2.5) constitute a molecular-field type of free energy where some of the coefficients are temperature dependent.

A quasi-one-dimensional model for incommensurate phases has been studied from a somewhat more general point of view in Ref. 24. Although there are some common aspects, that model differs from the present one in many details. In fact, the details are, as we shall see, to a large extent essential to describe the experimental situation in thiourea.

The stable configuration of the molecular displacements is achieved when forces acting on each molecule vanish, i.e.,

$$-\frac{\partial F}{\partial\varphi(\begin{smallmatrix}m\\ \kappa\end{smallmatrix})}=0 . \tag{2.8}$$

At that state the free energy F reaches a minimum. This condition is used in Sec. III in order to find numerically the exact stable configuration of all displacements $[\varphi(\begin{smallmatrix}m\\ \kappa\end{smallmatrix})]$.

The parameters a,h,b are described by the interaction of all atoms in the crystal, those in the (a,c) plane and those along the chain. The parameter a is a harmonic force constant. The extremum at $\varphi(\begin{smallmatrix}m\\ \kappa\end{smallmatrix})=0$ of the single-particle potential $V(\varphi(\begin{smallmatrix}m\\ \kappa\end{smallmatrix}))$ is not fixed by any symmetry element of the crystal. The third-order anharmonic term in V accounts for the following facts. First, the local potential $V(\varphi(\begin{smallmatrix}m\\ \kappa\end{smallmatrix}))$, being partly an effective interaction potential within the (a,c) plane, is not necessarily symmetric in $\varphi(\begin{smallmatrix}m\\ \kappa\end{smallmatrix})$ and hence the lowest admitted asymmetric term is $h\varphi^3(\begin{smallmatrix}m\\ \kappa\end{smallmatrix})$. Second, one sees from Fig. 3 that the centers of rotations of two neighboring molecules 1 and 4 are out of the b axis. Therefore, a simultaneous rotation of both molecules to the right leads generally to different interacting forces than a rotation of both molecules to the left. The term $h\varphi^3(\begin{smallmatrix}m\\ \kappa\end{smallmatrix})$ is the only one which will take this effect into account. Notice, however, that if a rotation of the molecule 1 to the right increases the energy, a rotation of the molecule 2 in the second chain and in the same direction decreases the energy. The term $h\varphi^3(\begin{smallmatrix}m\\ \kappa\end{smallmatrix})$ agrees also with the symmetry requirements of the $\hat{\tau}_4$ irreducible representation and corresponds to the third-order umklapp term.

The $SC(ND_2)_2$ molecule has a permanent dipole moment which lies along its twofold-symmetry axis. Consequently, part of the intermolecular interaction is of dipole-dipole type:

$$V_{\rm dip}=\frac{d_1d_2}{R^3}\cos\gamma(1,2)-\frac{3(\vec{d}_1\cdot\vec{R})(\vec{d}_2\cdot\vec{R})}{R^5} . \tag{2.9}$$

Here R is the distance between two molecules 1 and 2, $\gamma(1,2)$ is the angle between the dipoles $\vec{d}_1$ and $\vec{d}_2$. Owing to the one-dimensional character of the model and due to the fact that the molecules are in planes perpendicular to the b axis, only the first term of Eq. (2.9) contributes to the interaction. Calculating its second and fourth derivatives with respect to the angles, one finds the harmonic and the anharmonic force constants as expansion coefficients in a Taylor series:

$$\alpha_p=-(-1)^p\frac{d^2}{2R_p^3} , \tag{2.10a}$$

$$\beta_p=(-1)^p\frac{d^2}{24R_p^3} , \tag{2.10b}$$

where $R_p=|p|b_0/2$ is the distance to the pth neighbor. The quantity d^2/R_1^3 is treated as a fitting parameter. In this manner one calculates the harmonic force constants α_p, Eq. (2.10a) for the neighbors $p=3,4,\ldots,9$ and the anharmonic force constants β_p, Eq. (2.10b) for $p=2,3,4,\ldots,9$. It is necessary to take into account so many harmonic force constants because only then the minimum of the phonon dispersion curve can be obtained at about $k_m=0.16$. The values of the harmonic force constants a,α_1,α_2 and of the parameter d^2/R_1^3 were found from fitting the dispersion curve [see Sec. III, Eq. (3.7)] to four phonon frequencies[15] measured at a temperature close to the paraelectric-incommensurate phase transition.

The four points are indicated in Fig. 4.

The force constants depend on temperature and pressure. A simple approach which takes into account the temperature dependence of harmonic force constants is the pseudoharmonic theory. According to it, the largest effect of renormalization occurs for those force constants which correspond to small intermolecular distances where the potential changes drastically. On the other hand, for long-range potentials, such as the dipole-dipole interaction, the renormalization effect is negligible. Therefore the assumption is made below that all force constants, harmonic and anharmonic ones, are temperature independent, with the one exception that the force constant α_1 between nearest-neighbor molecules depends on temperature: $\alpha_1=\alpha_1(T)$. Here the short-range potentials, i.e., the repulsive forces and the hydrogen bonds between sulfur and deuterium may produce changes in the temperature range of the incommensurate phase.

Since it is not our aim here to derive the free energy [Eqs. (2.3)—(2.5)] from a microscopic force model, we restrict ourselves to the following conclusions about α_1. From the fit to the experimental phonon dispersion it follows that α_1 is negative and that in absolute value α_1 decreases with increasing temperature. Finally in all our calculations it will be assumed that any temperature dependence of the results follows from the temperature dependence of the nearest-neighbor harmonic force constant α_1.

The remaining fourth-order anharmonic force constants b and β_1 were estimated from two requirements: First, that the free energy of the incommensurate and the ferroelectric phases obtained by the numerical method should be equal in the vicinity of $k_m=\frac{1}{9}$; second, that the highest ratio of the third harmonic to the first one, $\eta_4(3k_m)/\eta_4(k_m)$, is about 0.2. Both requirements can be fulfilled only when b is positive, which means that the local potential becomes harder for larger displacements.

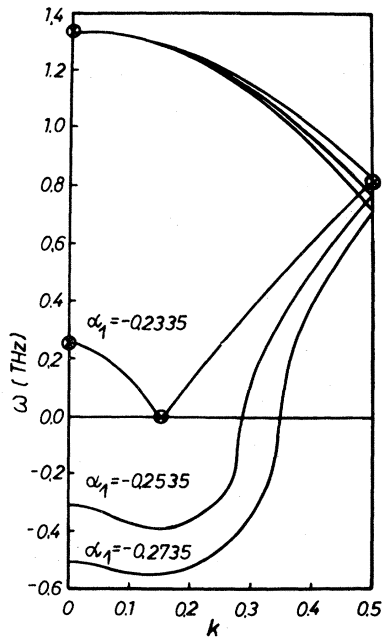

FIG. 4. Phonon dispersion curve calculated with Eq. (3.7) for several values of the force constant α_1.

Since the present model of thiourea is only one dimensional, no attempt has been made to reproduce the experimental data exactly. The aim was to find the microscopic configurations of molecular displacements and to relate them to the different macroscopic properties of thiourea. We should remember, however, that the results may change when another set of parameters, especially fourth-order anharmonic force constants, will be chosen. The numerical values of parameters of the model free energy [(2.3)—(2.5)] used in the calculations are listed in Table I.

III. APPROXIMATE SOLUTION

In the following sections we refer to the results of the numerical solutions of the one-dimensional model of thiourea. Before looking for the exact configurations of the incommensurate and ferroelectric phases, it is useful first to write explicitly a simple incommensurate solution of the linear chain model [Eqs. (2.3)—(2.5)] in terms of the first harmonic of $\hat{\tau}_4$ symmetry:

$$\varphi\binom{m}{\kappa}=(-1)^{\kappa}\eta_4(k)\cos[2\pi k(mb_0+r_\kappa-n_\epsilon b_0/2)] , \tag{3.1}$$

where the phase shift n_ϵ is defined by

$$\epsilon_4(k)=2\pi k n_\epsilon b_0/2 . \tag{3.2}$$

The values of $\eta_\epsilon=1$ and 2 correspond to the shift of the modulation wave by $b_0/2$ and b_0, respectively.

The solution (3.1) plays a role of initial conditions for the numerical calculation. Substituting this ansatz into Eq. (2.3), one can rewrite the free energy in the general form

$$F=\frac{1}{2N}\sum_{n=1}^{2N}\Lambda(2\pi k(n-n_\epsilon)b_0/2) , \tag{3.3}$$

where

$$\Lambda(2\pi k(n-n_\epsilon)b_0/2)=\Lambda(2\pi k(n-n_\epsilon)b_0/2+2\pi m_1 kl) , \tag{3.4}$$

with $m_1=0,\pm1,\pm2,\ldots$, as a periodic function which can easily be calculated explicitly. The values of $\Lambda(2\pi k(n-n_\epsilon)b_0/2)$ for n belonging to the second $(l,2l)$, third $(2l,3l)$, and following periods of the modulation, where l is the period of modulation, can be mapped onto the first one $(0,l)$. As a result of this procedure and for N sufficiently large, the discrete function $\Lambda(2\pi k(n-n_\epsilon)b_0/2)$ becomes a continuous distribution

TABLE I. Parameters of the one-dimensional model of thiourea.

a	1.80	b	0.150
α_2	−0.030825	β_1	0.008621
α_3	0.012249	β_2	0.002569
d^2/R_1^3	0.661440		

$\Lambda(2\pi k(x-n_\epsilon)b_0/2)$, and consequently, the free energy can be calculated as an integral

$$F=\frac{1}{\lambda}\int_0^\lambda dx\,\Lambda(2\pi k(x-n_\epsilon)b_0/2)\,, \tag{3.5}$$

where $\lambda=2l/b_0$. The integration is performed over one period of the function Λ, and therefore the free energy F does not depend on the phase n_ϵ.

Converting the summation over n in expression (3.3) into the integral (3.5), one finds

$$F=\tfrac{1}{2}\omega^2(k)\eta_4^2(k)+\tfrac{3}{8}C(k)\eta_4^4(k)\,, \tag{3.6}$$

where

$$\omega^2(k)=a+4\sum_{p=1}^{P}\alpha_p[1-(-1)^p\cos(2\pi kpb_0/2)]\,, \tag{3.7}$$

$$C(k)=b+8\sum_{p=1}^{P}\beta_p[1-(-1)^p\cos(2\pi kpb_0/2)]^2\,. \tag{3.8}$$

For our choice of model parameters (Table I) the phonon dispersion curve (3.7) is drawn in Fig. 4. The condition of extremum of the free energy $\partial F/\partial\eta_4(k)=0$ produces two solutions: primary,

$$\eta_4^2(k)=0,\quad F=0\,, \tag{3.9}$$

and secondary,

$$\eta_4^2(k)=-\frac{2\omega^2(k)}{3C(k)},\quad F_{\cos}=-\frac{\omega^4(k)}{6C(k)}\,. \tag{3.10}$$

The first corresponds to the paraelectric, the second to the incommensurate phase. The incommensurate configuration occurs for a wave vector k_m which is a solution of equation $\partial F/\partial k=0$.

In the ferroelectric phase, the configuration of the molecules can be written as

$$\varphi\binom{m}{\kappa}=(-1)^\kappa\eta_4(0)\,. \tag{3.11}$$

The free energy (2.3) with notation $F_f\equiv F_{\text{ferro}}$ is

$$F_f=a\eta_4^2(0)+b\eta_4^4(0)+8\eta_4^2(0)\sum_{p=1}^{P}{}'\alpha_p+32\eta_4^4(0)\sum_{p=1}^{P}{}'\beta_p\,, \tag{3.12}$$

where the summations $\sum'^{P}_{p=1}$ are confined to odd values $p=1,3,\ldots$. The equilibrium amplitude and the free energy of the ferroelectric phase are given by

$$\eta_4^2(0)=-\frac{1}{2}\frac{\omega^2(0)}{C(0)},\quad F_f=-\frac{1}{4}\frac{\omega^4(0)}{C(0)}\,, \tag{3.13}$$

where $C(0)$ and $\omega^2(0)$ must be calculated with Eq. (3.7) and (3.8), respectively, by setting $k=0$. Note that the limit for infinitely long wavelength ($k\to0$) calculated from expressions (3.10) differs from the results given by Eq. (3.13). Their ratios are

$$\frac{\eta_4(0)}{\eta_4(k=0)}=\frac{3}{4},\quad \frac{F_f}{F_{\cos}(k=0)}=\frac{3}{2}\,. \tag{3.14}$$

This apparently strange result becomes obvious when one recollects that the incommensurate free energy $F_{\cos}(k=0)$ is still described by the infinitely long wave and cannot be continuously transferred to the ferroelectric phase expression (3.12). Moreover, the value of the free energy depends on the order, whether one takes first the limit $k\to0$ or the integral.

IV. METHOD OF NUMERICAL SOLUTION

For a given value of the incommensurate wave number k_m and of the phase n_ϵ, the stable configuration of the molecules which corresponds to a minimum value of the model free energy Eqs. (2.3)–(2.5) can be found numerically. The calculations have been done for the chain of 1008 molecules ($N=504$ lattice constants b_0) with periodic boundary conditions. With this number of molecules it is possible to adjust to the chain the modulation waves which correspond to the commensurate phases $k_0=\frac{1}{7}$, $\frac{1}{8}$, and $\frac{1}{9}$. So, for example, the modulation waves $kb_0=\frac{1}{8}$ and $kb_0=\frac{1}{9}$ cover the whole chain by 63 and 56 periods, respectively. It is also possible to apply a modulation wave which covers the chain by any other integer number of periods, for example, 62. Although the last wave is, in principle, commensurate, we shall treat it later as incommensurate. This assumption can be easily accepted in the region where the lock-in phases are separated by truly incommensurate phases. The performed calculations showed also that the points of the free energies for such "incommensurate" wave vectors form smooth curves like the example in Fig. 9.

The system is given by the free energy. Replacing the $\varphi\binom{m}{\kappa}$ by φ_n, where

$$n=2m-1+\kappa\,, \tag{4.1}$$

one can write the free energy [(2.3)–(2.5)] with the aid of definitions (2.6) and (2.7) in the form

$$F=\frac{1}{2N}\sum_{n=1}^{2N}\Bigg[a\varphi_n^2+h\varphi_n^3+b\varphi_n^4+\sum_{p=1}^{P}\{\alpha_p[(\varphi_n-\varphi_{n-p})^2+(\varphi_n-\varphi_{n+p})^2]+\beta_p[(\varphi_n-\varphi_{n-p})^4+(\varphi_n-\varphi_{n+p})^4]\}\Bigg]\,, \tag{4.2}$$

where $N=1008$. In the numerical calculations we try to find such configurations of molecules $\{\varphi_n\}$ which give the smallest free energy F at a given external condition. To do so, we construct in the computer the configuration $\{\varphi_n\}$ of all 1008 molecules in the form of a simple cosine wave (3.1) of a desired wavelength $l=1/k$, phase n_ϵ, and

the normal amplitude $\eta_4(k)$ calculated from (3.10).

Next, the force acting on each molecule n has been calculated from the derivative of the free energy (4.2)

$$-\frac{\partial F}{\partial \varphi_n}=-2a\varphi_n-3h\varphi_n^2-4b\varphi_n^3 -4\sum_{p=1}^{P}\{\alpha_p[(\varphi_n-\varphi_{n-p})+(\varphi_n-\varphi_{n+p})] +2\beta_p[(\varphi_n-\varphi_{n-p})^3+(\varphi_n-\varphi_{n+p})^3]\} . \tag{4.3}$$

Then each molecule was shifted proportionally to the force (4.3) so that the new positions φ_n' were related to the old ones by

$$\varphi_n'=\varphi_n+\sigma\left[-\frac{\partial F}{\partial \varphi_n}\right] . \tag{4.4}$$

The coefficient $\sigma=0.09$ was chosen such that it ensured the convergence of the procedure in a reasonable time. The process (4.4) was repeated usually 100–1000 times. At the end, the forces $-(\partial F/\partial\varphi_n)$ experienced by each molecule were zero. The free energy (4.2) calculated during the iteration procedure was monotonically decreasing and at the end successive changes were inferior to $10^{-4}\%$.

In principle, owing to the boundary conditions, the system was unable to change the modulation wavelength during the calculations. At the end of each run the stable displacements φ_n of all molecules were established. Other initial conditions were also tested, in particular, a first-harmonic cosine wave (3.1) modulated with the second harmonic of smaller amplitude. After a long run the same configuration was reached as with the initial conditions in the form of the first harmonic only.

Any stable configuration of molecules can be analyzed by means of the expansion over harmonic and phases of symmetry $\hat{\tau}_1$ and $\hat{\tau}_4$:

$$\varphi_n=\sum_{j\geq 0}\{\eta_1(jk)\cos[2\pi jknb_0/2-\epsilon_1(jk)] +(-1)^n\eta_4(jk)\cos[2\pi jknb_0/2-\epsilon_4(jk)]\} . \tag{4.5}$$

To visualize the results we shall calculate the amplitudes of the harmonics

$$\eta_\nu^2(jk)=\frac{1}{N^2}\left[\left[\sum_{n=1}^{2N}\varphi_n(-1)^{(\nu-1)n}\cos(2\pi jknb_0/2)\right]^2 +\left[\sum_{n=1}^{2N}\varphi_n(-1)^{(\nu-1)n}\sin(2\pi jknb_0/2)\right]^2\right] \tag{4.6}$$

and the phases

$$\tan\epsilon_\nu(jk)=\frac{\sum_{n=1}^{2N}\varphi_n(-1)^{(\nu-1)n}\sin(2\pi jknb_0/2)}{\sum_{n=1}^{2N}\varphi_n(-1)^{(\nu-1)n}\cos(2\pi jknb_0/2)} . \tag{4.7}$$

The phases are specified by Eq. (4.7) modulo π. π should be added to $\epsilon_\nu(jk)$ if the sign of the denominator of Eq. (4.7) is negative.

Also, two effects are worth mentioning for the case when the external conditions correspond to the lock-in phase. First, if one starts with the cosine modulation characterized by the phase n_ϵ which does not correspond to the minimum of pinning free energy, then the modulation wave changes its phase so that at the end of the calculation the free energy reaches the minimum. However, this process has rather long relaxation time of an order of 2000 time steps. Second, starting from such α_1 and h, which correspond to the lock-in region and using initial conditions with the wave vector k close to the lock-in value, one finds after a long run of 2000 steps a final configuration which consists of the region of commensurate lock-in structure and incommensurate defects. The system goes over from the initially incommensurate modulation to the locally commensurate one. It cannot get rid of the defects that have arisen because of the periodic boundary conditions.

V. NUMERICAL RESULTS

Here we shall discuss the results of the numerical calculations of the free energy (4.2) for the various choices of the values of the parameters k, α_1, h, and n_ϵ:

$$F=F(2\pi k,\alpha_1,h,n_\epsilon) . \tag{5.1}$$

The remaining parameters are taken fixed with the values given in Table I.

A. Case $h=0$

The values of F for discrete values of k (measured in units b_0^{-1}) lie on the curve with a single minimum. The values of the free energy at the minimum $F_m=F(2\pi k_m,\alpha_1,0,n_\epsilon)$ and the position of the minimum k_m, as a function of α_1, are shown in Figs. 5 and 6, respectively. The results show that within the accuracy of our calculations the free energy F_m for $h=0$ does not depend on the phase n_ϵ for any value of α_1 and k including the commensurate values $\frac{1}{7}$, $\frac{1}{8}$, and $\frac{1}{9}$. In other words, no lock-in phases appear in the model without the asymmetric field h.

The free energy of the ferroelectric phase calculated with the use of Eq. (3.12) and the free energy $F_{\cos}$ of the incommensurate phase with one cosine modulation [Eq. (3.10)] are also shown in Fig. 5. The value of $F_{\cos}$ is given at its absolute minimum. The position of that minimum is also indicated in Fig. 6. The behavior of the free energies as a function of α_1 shows that the phase transition from the paraelectric to the incommensurate phase at $\alpha_1(T_c)=-0.237$ is of second order while that from the incommensurate to the ferroelectric phase at $\alpha_1(T_0)=-0.2720$ is of first order. One can notice that

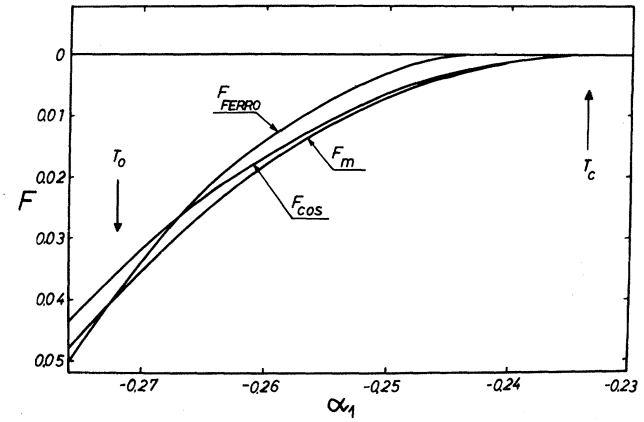

FIG. 5. Free energies with $h=0$ as function of α_1. F_m is the value at the absolute minimum obtained from numerical calculations. $F_{\cos}$ corresponds to expression (3.10) at the absolute minimum.

$\alpha_1(T)$ changes in the whole region of the incommensurate phase by 15%. Such changes are to be expected in thiourea, since α_1 is described by short-range forces including the hydrogen bond.

When lowering α_1 (or equivalently T), one can observe the increase of the difference between the free energy $F_{\cos}$ and the true free energy F_m. This effect is due to squaring of the modulation wave. It means that the cosine-type incommensurate wave, which appears just below the phase-transition point from the paraelectric phase, becomes gradually similar to the periodic steplike function.[25–28] This process is accompanied by an increase of the wavelength of the incommensurate phase, which is indicated in Fig. 6. There too one can notice that the difference between the wave vectors for a simple solution with a single cosine modulation and the exact solution increases while the temperature is lowered. The calculated periodic and stable configuration of molecules in thiourea can be analyzed by

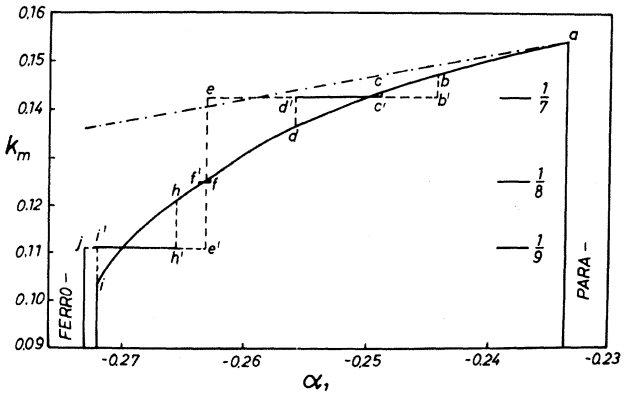

FIG. 6. Modulation wave vector of the incommensurate and lock-in phases as a function of α_1. The curves *abcdhi*, *acc'd'dff'hh'i'i*, and *abb'ee'j* correspond to $h=0$, $h=0.015$, and $h=0.1$, respectively. The line (—·—) denotes the minimum of the phonon dispersion curve (3.7).

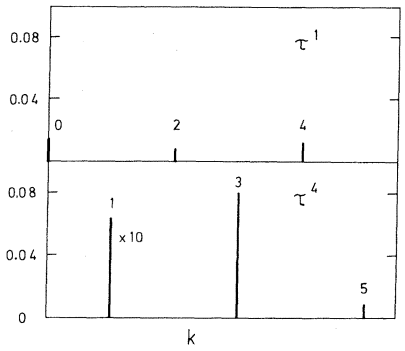

FIG. 7. Amplitudes of normal harmonics $\eta_1(jk)$ and $\eta_4(jk)$ of symmetry $\hat{\tau}_1$ and $\hat{\tau}_4$, respectively, of the incommensurate configuration with $\alpha_1=-0.262$, $k_m=0.127$, $h=0.05$.

an expansion into harmonics $\eta_\nu(jk)$, Eq. (4.5). Then one finds that when $h=0$, the even harmonics of symmetry $\hat{\tau}_4$ and all harmonics of symmetry $\hat{\tau}_1$ are absent. The harmonics of symmetry $\hat{\tau}_4$ decrease with increasing index j as is shown in Fig. 7. The functions $\eta_4(jk_m)$ increase with decreasing α_1 or equivalently with decreasing temperature (Fig. 8). With a diminishing value of α_1, the third and fifth harmonics $\eta_4(3k_m)$ and $\eta_4(5k_m)$, respectively, increase much faster than the first one. That indicates that the squaring effect also increases with decreasing temperature.

The phases $\epsilon_4(jk)$ of the incommensurate modulation were calculated with the relation (4.7). Each phase of higher harmonic proves to be a multiple of the phase of the first harmonic. We have found that

$$\epsilon_4(3k)=3\epsilon_4(k)-\pi \quad \text{and} \tag{5.2}$$

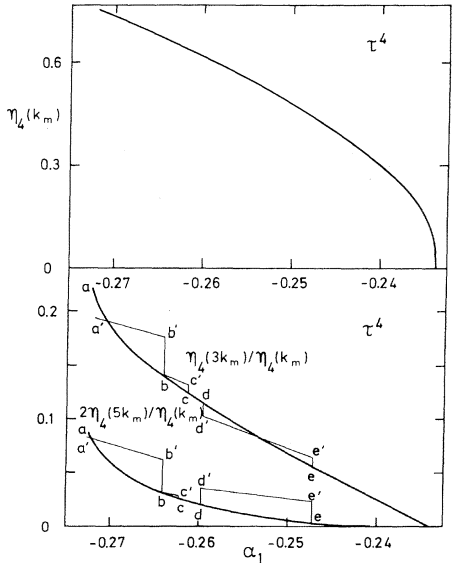

FIG. 8. Upper panel, amplitude of first harmonic of symmetry $\hat{\tau}_4$ at the wave vector k_m as a function of α_1 for $h=0$. Lower panel, ratios of third and fifth harmonics of symmetry $\hat{\tau}_4$ to the first one. The *abcde* and *a'b'b'c'd'e'e* curves correspond to $h=0$ and $h=0.05$, respectively.

$$\epsilon_4(5k)=5\epsilon_4(k)\ ,$$

for any values of k and α_1.

In this case, taking into account Eqs. (3.2), (4.5), and (5.2), we can rewrite the modulated wave as

$$\varphi_n=\sum_{j\,(>0)}(-1)^n\eta_4(jk)(-1)^{q_j}\times\cos[2\pi jk(n-n_\epsilon)b_0/2]\ , \tag{5.3}$$

where $q_j=0,1,0$ for $j=1,3,5$, respectively. Since n_ϵ is arbitrary, any shift of the modulation wave is possible. This is in agreement with the well-known symmetry properties of the incommensurate state.[29,30]

B. Case $h\neq 0$

The numerical solution of the one-dimensional model [(2.3)—(2.5)] with a nonzero value of the coefficient h of the third-order terms leads to new phenomena. The free energy (5.1) as a function of k has two kinds of solutions: the continuous curves which correspond to the incommensurate configurations and the isolated points which occur for the commensurate values $\frac{1}{7}$, $\frac{1}{8}$, and $\frac{1}{9}$. Figure 9 shows the case when the free energy at $\frac{1}{7}$ is lower than the incommensurate values. The system incorporates the configuration which has the lowest free energy. If it is the isolated point, then the system goes over into one of the lock-in phases $\frac{1}{7}$, $\frac{1}{8}$, or $\frac{1}{9}$. One sees that the phase transition from the incommensurate to the lock-in phase is always of first order. This fact agrees with experiment.[15]

The values of the free energy at the commensurate points seem to be a function of the initial phase n_ϵ at which the numerical minimalization procedure started, provided the short run is used (100 time steps). Allowing the computer to make at least 1000 time steps, one observes slow variation of the phase which approaches the value of the stable phase n_ϵ of the commensurate modulation. The short runs then allow one to get some insight into the approximate form of the phase dependence of the free energy $F(n_\epsilon)$ and related unstable configuration of the molecules. Under these conditions one finds the following.

The common feature of the $\frac{1}{7}$ and $\frac{1}{9}$ lock-in phases is that their free energies are periodic with one lattice constant (Fig. 10). Examples of those molecular configurations are shown in Figs. 11 and 12. The configuration for $k=0.113$ close to the commensurate value $k=\frac{1}{9}\approx 0.111$ shows that the pattern of modulation changes systematically when one travels along the chain. For all commensurate values the pattern of displacements is the same for each period of modulation. At the lock-in phase $k=\frac{1}{9}$ and $n_\epsilon=0$, eight molecules have a negative position. The asymmetric term $h\varphi_n^3$ contributes then remarkably to the lowering of the free energy, and it is not totally balanced by the remaining ten molecules having positive position. The shift of the modulation wave by half a lattice constant reverses the configuration and leads to an increase in the free energy above the incommensurate value for the neighboring values of k. One also notices that the configurations $k=\frac{1}{9}$, $n_\epsilon=0$ and $k=\frac{1}{7}$, $n_\epsilon=1$ are similar in structure. Both correspond to the minimum of the free energy.

The configuration in the commensurate phase $k=\frac{1}{8}$ shown in Fig. 12, periodic with half a lattice constant (Fig. 10), exhibits quite different properties. At zero asymmetric field h the two halves of the period show an inverse configuration. With increasing $h\neq 0$, the length of the first half of the modulation period starts to be different from the second one. This asymmetry increases with increasing h. It also means that the $\frac{1}{8}$ lock-in phase has a permanent dipole moment. Since the zeroth-order harmonic is nonzero for the $\frac{1}{8}$ phase, the spontaneous polarization is proportional to the asymmetric field h.[31]

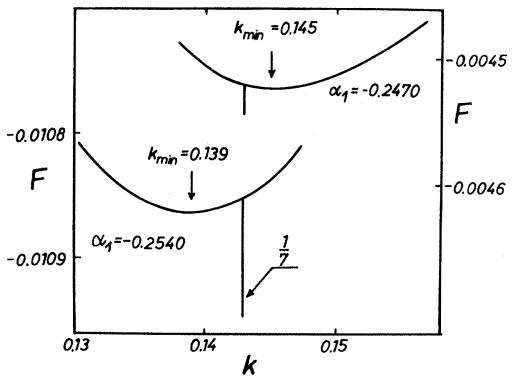

FIG. 9. Free energy as a function of wave vector for different α_1. The values at $k=\frac{1}{7}$ correspond to F of the lock-in phase with $h=0.1$.

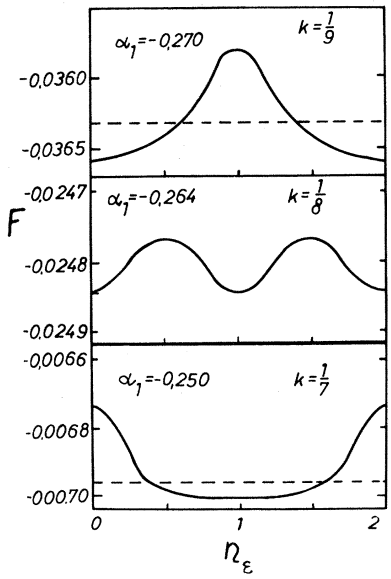

FIG. 10. Free energy as a function of the phase n_ϵ at $h=0.1$ for $\frac{1}{9}$, $\frac{1}{8}$, and $\frac{1}{7}$ lock-in phases. Dotted lines indicate the level of the free energy for the incommensurate value of the wave vector which is close to the relevant commensurate value.

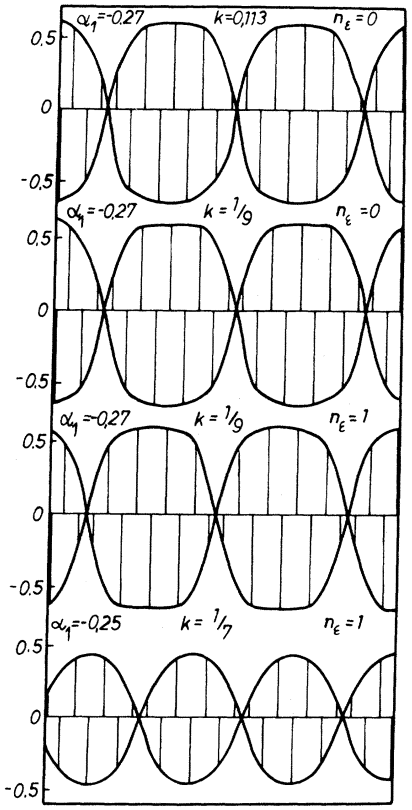

FIG. 11. Amplitudes φ_n for few molecules along the chain at $h=0.1$.

Nonzero values of the zeroth-order harmonic involve in this case nonzero values of the even harmonics.

The temperature dependence, or rather the α_1 dependence, of the modulation wave vector in the presence of the asymmetric field is given in Fig. 6. Within the accuracy of our numerical calculations, the minimum k_m of the free energy of the truly incommensurate phase does not depend on the value of the asymmetric field h and is the same as for $h=0$. The existing differences are entirely due to the appearance of the isolated points of the lock-in phases. In Fig. 6 the wave vector k_m at some discrete values of α_1 changes drastically from one value of k_m to a different one. At these points the absolute minimum of the free energy switches from one phase to another one. The steplike behavior of k_m as a function of α_1 does not take into account the fluctuations in the system. To some extent the fluctuations might smooth out the calculated curves. The stepwise behavior of the modulation wave vector k_m as a function of temperature or other parameters is a subject of considerable theoretical interest.[19,32,33]

The calculations of the modulation wavelength k_m of the stable configuration as a function of α_1 carried out for several values of h have given us the opportunity to sketch the phase diagram of the one-dimensional model [(2.3)–(2.5)]. The phase diagram, shown in Fig. 13, indicates the most stable configuration at a given value of α_1, the temperature, and h, the asymmetric field. The wave vector of the modulation of the incommensurate regions of the phase diagrams for any value of h is given by the solid line of Fig. 6. Different properties of odd and even lock-in phases are also seen from the phase diagram. The region of $\frac{1}{7}$ and $\frac{1}{9}$ phases are much wider than that of $\frac{1}{8}$. For larger values of h, the $\frac{1}{8}$ phase is consumed by the neighboring lock-in phases.

The Fourier analysis (4.5) of the stable configuration in the presence of the asymmetric field h leads to results similar to those obtained for the case $h=0$. An example of the harmonics for the incommensurate phase is shown in Fig. 8. The even harmonics of symmetry $\hat{\tau}_4$ and odd harmonics of symmetry $\hat{\tau}_1$ are still absent. Now, however, due to the presence of the asymmetric field h, one observes the even-order harmonics of symmetry $\hat{\tau}_1$. The amplitudes of these harmonics are proportional to h and are small, as can be seen from Fig. 8. The amplitude of the first-order harmonic $\eta_4(k_m)$ of symmetry $\hat{\tau}_4$ as a function of α_1 shows almost the same behavior as for $h=0$, Fig. 7. Some differences appear for the ratios of the third and the fifth harmonics of symmetry $\hat{\tau}_4$ to the first one. Discontinuous behavior for $h\neq 0$ results from transitions to the different lock-in phases.

The phases $\epsilon_4(jk)$ of the symmetry $\hat{\tau}_4$ have also been calculated according to (4.7). For the incommensurate modulation we have found the same results (5.2) as for the case $h=0$. Moreover, at the minimum of the free energy of the commensurate modulation $\frac{1}{7}$, $\frac{1}{8}$, and $\frac{1}{9}$, the calculated values of the phases agree as well with the previous

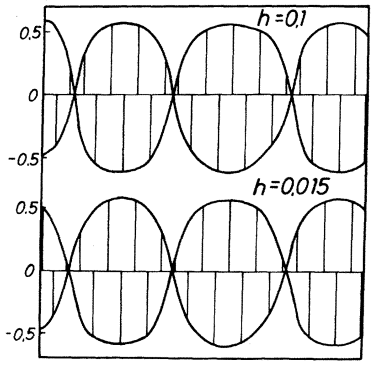

FIG. 12. Amplitudes φ_n for few molecules along the chain at $\varphi_1=-0.2640$, $k=\frac{1}{8}$, and $n_\epsilon=0$.

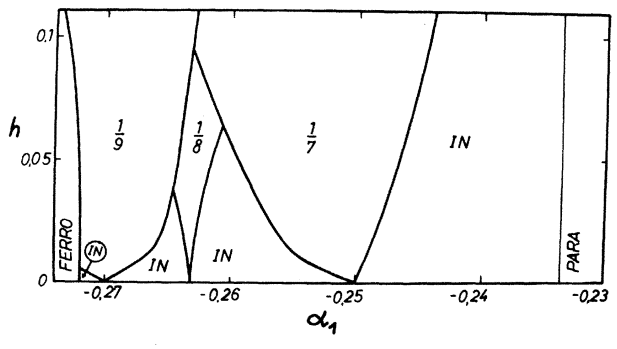

FIG. 13. h-α_1 phase diagram of the model.

results (5.2) for any set of k, α_1 and $h \neq 0$. The free energy for the values of the wave vector not equal to $\frac{1}{7}$, $\frac{1}{8}$, or $\frac{1}{9}$ still does not depend on the phase n_ϵ. Starting from the initial conditions in form of the cosine function (3.1) with $k = \frac{1}{2}b_0$, it was easy to generate the ferroelectric phase.

VI. HARMONIC ANALYSIS OF THE FREE ENERGY

Higher harmonics play the role of a secondary order parameter.[34,35] In order to obtain a systematic description of the free energy in terms of harmonics, we first introduce the normal modes of the one-dimensional model.

The configuration of the static displacements of the molecules can be analyzed with the aid of the normal amplitudes $\rho_\nu(k_j)$ as follows:

$$\varphi\binom{m}{\kappa} = \sum_{k_j} \sum_{\nu=1,4} \rho_\nu(k_j) e_\kappa(k_j,\nu) \exp(2\pi i k_j m b_0) , \tag{6.1}$$

where k_j is the wave vector labeled by the index j.

The index $\nu = 1,4$ labels the symmetry of $\hat{\tau}_1(k_j)$ or $\hat{\tau}_4(k_j)$ of the normal amplitude $\rho_\nu(k_j)$, respectively. The $e_\kappa(k_j,\nu)$ are the polarization vectors.

The summation over k_j in (6.1) is restricted to special discrete values of the wave vectors. It follows from the assumption that the incommensurate modulation is a periodic function with a period l, where l/b_0 is not necessarily rational. From (6.1) one finds that the only nonzero values of the normal amplitudes are

$$\rho_\nu(k_j) = \rho_\nu(jk), \quad \text{where } j = 0, \pm 1, \pm 2 , \tag{6.2}$$

and $k = 1/l$. The first harmonics ($j = \pm 1$) of symmetry $\hat{\tau}_4$ which produce the incommensurate structure should be characterized by the wave vector k from the positive half of the first Brillouin zone, i.e., $0 \leq k \leq \frac{1}{2}b^*$, where $b^* \equiv 1/b_0$. All other harmonics relevant for the analysis are chosen as a multiple of the first one according to the relation (6.2). Hence the summation over all k_j in (6.1) must be reduced to the integer indices of the harmonics only. The summation over j runs from $-\infty$ to ∞ and from $-L+1$ to L for incommensurate and commensurate modulations, respectively. In the latter case, Lb_0 is the commensurate period of modulation. Since in thiourea only harmonics up to fifth order ($j = \pm 5$) play an essential role, one can use the same expansion (6.1) with $k_j = jk$ for incommensurate and commensurate phases.

The polarization vectors of the two symmetries $\hat{\tau}_1$ and $\hat{\tau}_4$ are

$$e_\kappa(jk,\nu) = \frac{1}{\sqrt{2}} (-1)^{(\nu-1)\kappa} \exp(2\pi i j k r_\kappa) , \tag{6.3}$$

with $\nu = 1$ or $\nu = 4$, respectively. Here again [compare Eq. (2.2)] r_κ is 0 or $b_0/2$, depending on whether $\kappa = 0$ or 1, respectively. The polarization vectors are orthonormalized and complete.

The irreducible representations $\hat{\tau}_1(jk)$ and $\hat{\tau}_4(jk)$ of the star $k_7 = (0,jk,0)$ of the paraelectric space group D_{2h}^{16} have a peculiar property. Each of these representations can be identified with the other one labeled with the wave vector shifted by a reciprocal-lattice vector b^*:

$$\hat{\tau}_1(jk) = \hat{\tau}_4(jk \pm b^*) . \tag{6.4}$$

This property, appropriate for the three-dimensional thiourea crystal as well, is present in our one-dimensional model.

With the use of the expansion (6.1) and the relation (6.3), the free energy [(2.3)–(2.5)] can be expressed in terms of the normal amplitudes:

$$\begin{aligned} F = {} & \tfrac{1}{4} \sum_{j,j'=-\infty}^{\infty} \sum_{\nu,\nu'=1,4} \rho_\nu(jk)\rho_{\nu'}(j'k)[1+(-1)^M(-1)^{\nu+\nu'}]\Omega_{\nu\nu'}(jk,j'k)\delta((j+j')k - Mb^*) \\ & + \frac{1}{4\sqrt{2}} h \sum_{j,j',j''=-\infty}^{\infty} \sum_{\nu,\nu',\nu''} \rho_\nu(jk)\rho_{\nu'}(j'k)\rho_{\nu''}(j''k)[1-(-1)^{\nu+\nu'+\nu''}(-1)^M]\delta((j+j'+j'')k - Mb^*) \\ & + \tfrac{1}{8} \sum_{j,j',j'',j'''=-\infty}^{\infty} \sum_{\nu,\nu',\nu'',\nu'''} \rho_\nu(jk)\rho_{\nu'}(j'k)\rho_{\nu''}(j''k)\rho_{\nu'''}(j'''k) \\ & \times [1+(-1)^M(-1)^{\nu+\nu'+\nu''+\nu'''}] C_{\nu\nu'\nu''\nu'''}(jk,j'k,j''k,j'''k) \\ & \times \delta((j+j'+j''+j''')k - Mb^*) , \end{aligned} \tag{6.5}$$

where

$$\Omega_{\nu\nu'}(jk,j'k) = a + \sum_{p=-P}^{P} \alpha_p S_p(jk,\nu) S_p(j'k,\nu') , \tag{6.6}$$

$$C_{\nu\nu'\nu''\nu'''}(jk,j'k,j''k,j'''k) = b + \sum_{p=-P}^{P} \beta_p S_p(jk,\nu) S_p(j'k,\nu') S_p(j''k,\nu'') S_p(j'''k,\nu''') , \tag{6.7}$$

and

$$S_p(jk,\nu)=1-(-1)^{(\nu-1)p}\exp(-2\pi ijkpb_0/2)\ . \quad (6.8)$$

The values $M=0$ and $M=\pm1,\pm2,\ldots$ correspond to the normal and umklapp terms, respectively. It is worth pointing out that all second-, third-, and fourth-order terms of the free energy (6.5) are in agreement with the invariants constructed from relevant basic functions of $\hat{\tau}_1$ and $\hat{\tau}_4$ irreducible representations of star k_7 in Kovalev's notation[17] of the three-dimensional space group D_{2h}^{16}.[36] Thus the general form of the free energy for the three-dimensional crystal of thiourea will be the same. For displacive phase transitions, as in thiourea, the quantity $\Omega_{\nu\nu}(jk,-jk)$ can be treated as a square of the phonon frequency. In the first Brillouin zone $\hat{\tau}_4$ is the soft branch, but in the second Brillouin zone the role of the branches interchange and $\hat{\tau}_1$ becomes soft.

Often it is much more convenient to work with the real quantities rather than with the imaginary ones. In such an approach the imaginary normal amplitude $\rho_\nu(jk)$ can be represented by the real and positive harmonic $\eta_\nu(jk)\geq 0$ and the phase $\epsilon_\nu(jk)$:

$$\rho_\nu(0)=\sqrt{2}\eta_\nu(0)\cos\epsilon_\nu(0)$$
$$=\frac{1}{\sqrt{2}N}\sum_{m=1}^{N}\sum_{\kappa=0}^{1}\varphi\binom{m}{\kappa}(-1)^{(\nu-1)\kappa}\ , \quad (6.9a)$$

$$\rho_\nu(jk)=\frac{1}{\sqrt{2}}\eta_\nu(jk)\exp[-i\epsilon_\nu(jk)] \quad \text{if } jk\neq 0,b^*\ . \quad (6.9b)$$

Since the zeroth harmonic $\eta_\nu(0)$ measures a uniform displacement of the molecules, with no loss of the generality we can set

$$\epsilon_\nu(0)=0 \text{ or } \pi$$

and (6.10)

$$\rho_\nu(0)=\pm\sqrt{2}\eta_\nu(0)\ .$$

The two values of $\epsilon_\nu(0)$ correspond to two ferroelectric domains of thiourea. The configuration of the displacements can be expanded over harmonics and phases as

$$\varphi\binom{m}{\kappa}=\sum_{j\ (\geq 0)}\sum_{\nu=1,4}\eta_\nu(jk)(-1)^{(\nu-1)\kappa}$$
$$\times\cos[2\pi jk(mb_0+r_\kappa)-\epsilon_\nu(jk)]\ . \quad (6.11)$$

The free energy (6.5) can be expressed by the wave vectors k of the main modulation, the amplitudes, and the phases of the harmonics: $F=F(k,\eta_\nu(jk),\ldots,\epsilon_\nu(jk),\ldots)$, with $\nu=1,4$ and $j=1,2,3,\ldots$. The values of this set of parameters can be found from the conditions of extremum of the free energy

$$\frac{\partial F}{\partial k}=0\ , \quad (6.12a)$$

$$\frac{\partial F}{\partial \eta_\nu(jk)}=0\ , \quad (6.12b)$$

$$\frac{\partial F}{\partial \epsilon_\nu(jk)}=0\ . \quad (6.12c)$$

An explicit expression of the free energy will be given in the Appendix.

VII. DISCUSSION OF HARMONICS AND THEIR PHASES

The expansion (A1) contains those harmonics of symmetry $\hat{\tau}_4$ which are the largest and which reproduce all essential features of the model. The harmonic $\eta_1(2k)$ of symmetry $\hat{\tau}_1$ is included to indicate other possible couplings and lock-in terms. For our choice of parameters the numerical calculations showed that the second-order harmonic is small. It also contributes very little to the lock-in energies. Therefore, in Eq. (A1) we set $\eta_1(2k)=0$, and exclude this harmonic from the forthcoming discussion. Under these circumstances all umklapp terms are of the third order.

We start with a discussion of the incommensurate phase. Now the modulation wavelength l, expressed in the lattice constant units b_0, is not equal to any rational number and the third-order umklapp term does not play any role. By using the extremum condition (6.12b), we get for the first harmonic

$$\eta_4(k)=\pm\left[-\frac{2}{3}\frac{\Omega_{44}(k,-k)}{C_{4444}(k,k,-k,-k)}\right]^{1/2}\ . \quad (7.1)$$

Here $\Omega_{44}(k,-k)<0$, while $C_{4444}(k,k,-k,-k)>0$. In addition, we can express any higher-order harmonic by a product of lower harmonics. Repeating that process, one finds that $\eta_4(jk)\sim[n_4(k)]^j$ if j is odd. This property assures also that at the phase transition from the paraelectric to the incommensurate phase one observes not only the condensation of the first harmonic, but simultaneous condensation of all odd harmonics, although the intensity of the higher harmonics is small.

For even harmonics $\eta_4(0),\eta_4(2k),\ldots$, the situation is different. Lack of terms $\eta_4(0),\eta_4^3(k)$, $\eta_4(2k)\eta_4^3(k)$ leads, according to Eq. (6.12b), to the disappearances of all even harmonics. The zeroth harmonics $\eta_4(0)$ is proportional to the spontaneous polarization.[31] In the ferroelectric phase $\eta_4(0)$ is nonzero but vanishes in the incommensurate phase.

From the condition of the extremum of the free energy (6.12c) the following relations between the phases of the incommensurate modulation can be established:

$$\epsilon_4(jk)=j\epsilon_4(k)-q_j\pi \quad \text{for } j=1,3,\ldots\ . \quad (7.2)$$

Here q_j is either 0 or 1, and this value of q_j should be taken which lowers the free energy.[35] One notices that Eq. (6.12c) imposes no restriction on the phase $\epsilon_4(k)$ of the first harmonic. The incommensurate modulation can be shifted then by any value of the phase, without any variation of the free energy. In other words, the incommensurate modulation is not pinned. The wave vector k_m of the incommensurate modulation at which the free energy (A1)

achieves the minimum is described by the extremum condition (6.12a). Remembering that the harmonics $\eta_4(jk)$ are only indexed by the wave vector k, and using also Eq. (7.2), one finds

$$\frac{\partial F(k)}{\partial k}=\frac{1}{2}\frac{\partial\Omega_{44}(k,-k)}{\partial k}\eta_4^2(k)+\frac{1}{2}\frac{\partial\Omega_{44}(3k,-3k)}{\partial k}\eta_4^2(3k)+\cdots . \tag{7.3}$$

In this approach when $\eta_1(2k)=0$, none of the derivatives depends upon the asymmetric field h, therefore no h dependence of the wave vector k_m might be expected. This effect is confirmed by the numerical calculations in Sec. V.

We next consider the commensurate phases. In our simplified model, in which the second-order harmonic of symmetry $\hat{\tau}_1$ can be neglected, the lock-in phases arise because of the presence of the third-order umklapp terms in the free-energy expansion (A1). For particular commensurate wave vectors $k=\frac{1}{7},\frac{1}{8},\frac{1}{9}$ these terms contribute to the free energy. The δ functions ensure that these terms are present only when the sum of the modulation wave vectors of the relevant harmonics is equal to the reciprocal-lattice vector b^*. In the lock-in phases $\frac{1}{7}$ and $\frac{1}{9}$ the even harmonics are still zero. However, the third-order umklapp term contributes little to odd harmonics. In the lock-in phase $\frac{1}{8}$ one finds also a small contribution to the odd harmonics, the contribution which originates from the third-order umklapp term. The even-order harmonics become nonzero in the lock-in phase $\frac{1}{8}$ only. Again from the extremum condition one finds that these harmonics are proportional to the asymmetric field h.

In the commensurate phases the free energy does depend on the phases $\epsilon_4(jk)$. Shifting the modulation, however, by one lattice constant, one arrives at the same value of the free energy. Studying the conditions of extremum (6.12c), one finds the phases for which the free energy has a minimum. Provided $h>0$ and the fourth-order coefficients are positive, one obtains for the phase shift n_ϵ defined by Eq. (3.2) the following results: $n_\epsilon=1$ and $n_\epsilon=0$ for the lock-in phases $\frac{1}{7}$ and $\frac{1}{9}$, respectively, and $n_\epsilon=0$ and $n_\epsilon=1$ for two possible configurations $\epsilon_4(0)=0$ and $\epsilon_4(0)=\pi$, respectively, of the lock-in phase $\frac{1}{8}$. One sees then that the relation (7.2) between phases of different harmonics is valid not only for incommensurate phases, but also for commensurate phases at the extremum of the free energy. If one assumes for the commensurate phase the validity of (7.2) for any value of $\epsilon_4(jk)$, then one can find the phase dependence of the free energy. Substituting Eqs. (7.2) and (3.2) into the lock-in terms of (A1) and taking into account $\eta_1(2k)=0$, one finds the excess of the free energy. In particular $\Delta F_{1/7}$ is proportional to $h\delta(7k-b^*)\cos(\pi n_\epsilon)$, $\Delta F_{1/9}$ to $h\delta(9k-b^*)\cos[\pi(n_\epsilon+1)]$, and $\Delta F_{1/8}$ to $h\delta(8k-b^*)\cos[\pi(n_\epsilon+1)]$ for $\epsilon_4(0)=0$, and to $h\delta(8k-b^*)\cos(\pi n_\epsilon)$ for $\epsilon_4(0)=\pi$, respectively.

In each case the free energy as a function of the phase shift n_ϵ is periodic with one lattice constant ($n_\epsilon=2$). One notices, however, that the free energy of phase $\frac{1}{9}$ is shifted by half a lattice constant ($n_\epsilon=1$) with respect to the free energy of phase $\frac{1}{7}$ as shown in Fig. 10. For the phase $\frac{1}{8}$ there are two possibilities depending upon a choice at the domain: $\epsilon_4(0)=0,\pi$. Therefore the free energy of phase $\frac{1}{8}$ as a function of the phase n_ϵ has two minima as is shown in Fig. 10.

VIII. CONCLUSIONS

We have proposed and studied a one-dimensional model of the incommensurate and commensurate phases of crystalline thiourea. On the basis of this discrete model we have carried out numerical and analytical calculations.

Our main numerical results are the following. In absence of the asymmetric field h, the intermediate phase between the paraelectric and the ferroelectric phase is truly incommensurate while there is no trace of a lock-in phase. The temperature dependence of the incommensurate wave vector k_m is to a large extent produced by an increasing squaring effect of the initially sinusoidal modulation with lowering temperature. The increase of the squaring is reflected in the increase in amplitude of higher harmonics. The lock-in commensurate phases occur only at nonzero asymmetric field h. The $\frac{1}{7}$ and $\frac{1}{9}$ lock-in phases are similar in structure. The $\frac{1}{8}$ lock-in phase has different features as follows from the possible existence of two different domains. In the numerical calculations the model parameters were chosen such that the mode with $\hat{\tau}_4$ symmetry played an essential role. Odd harmonics with this symmetry were found to be of importance. With the present choice of parameters, harmonics of $\hat{\tau}_1$ symmetry are too small in order to contribute to the lock-in phases of the model.

In addition to the numerical calculations, we have performed an extensive analytical investigation. This analysis leads to conclusions that are in agreement with the results of the numerical calculations. Besides the role of the amplitudes $\eta_\nu(jk)$, we could also clarify the role of the phases $\epsilon_\nu(jk)$ in the commensurate and in the incommensurate phases. Here again the connection with the numerical results could be established.

The purpose of the numerical calculations was not to reproduce the experimental data exactly but to test—in absence of definite knowledge of the values of the force parameters a,b,h,α_p,β_p—the possibilities of the model. Therefore some quantitative disagreements with the available experimental data[15,25] can be noted. First, the numerical results exhibit a large region of the truly incommensurate phase between the paraelectric and the $\frac{1}{7}$ lock-in phase which is not observed at zero pressure, at least not in $SC(ND_2)_2$. In this respect the phase transition from the paraelectric to the incommensurate phase can be shifted down by appropriate changes of the values of the model parameters (Table I). Then the squaring effect around the modulation wave vector $\frac{1}{7}$ will be smaller and consequently the $\frac{1}{7}$ lock-in phase will be narrower. Next, the second-order harmonic of symmetry $\hat{\tau}_4$, which is well ob-

served in the diffraction experiment, is negligibly small in the numerical results. On the other hand, the third- and the fifth-order harmonic of symmetry $\hat{\tau}_4$ exhibit a too-large intensity. Again, this defect can be removed by an appropriate choice of the numerical parameters. Then however, the fourth-order umklapp terms of the free energy (A1), which contain the harmonic $\eta_1(2k)$, will contribute to the lock-in energies at phases $\frac{1}{7}$, $\frac{1}{8}$, and $\frac{1}{9}$. Consequently even in the absence of the asymmetric field h, the lock-in phases will be present.

ACKNOWLEDGMENTS

The authors wish to thank Mme. M. Lambert for drawing their attention to the problem of thiourea, and R. M. Pick for constructive criticism and stimulating comments. Further they have benefited from useful discussions with F. Denoyer, A. H. Moudden, P. Lederer, and J. Naudts. J. Fivez gave helpful advice for the numerical calculations. The work was financially supported by the Belgian Project Neutron Scattering.

APPENDIX

It is instructive to write explicitly the expansion of the free energy with those essential terms which contain the harmonics $\eta_4(0)$, $\eta_4(k)$, $\eta_4(2k)$, $\eta_4(3k)$, and $\eta_1(2k)$. As the numerical calculations showed, all other harmonics are small and can be neglected (Fig. 7). Therefore we retain

$$
\begin{aligned}
F = {} & \Omega_{44}(0,0)\eta_4^2(0)+\tfrac{1}{2}\Omega_{44}(k,-k)\eta_4^2(k)+\tfrac{1}{2}\Omega_{44}(2k,-2k)\eta_4^2(2k)+\tfrac{1}{2}\Omega_{44}(3k,-3k)\eta_4^3(3k) \\
& +\tfrac{1}{2}\Omega_{11}(2k,-2k)\eta_1^2(2k)+\tfrac{3}{4}h\eta_4(2k)\eta_4^2(3k)\cos[\epsilon_4(2k)+2\epsilon_4(3k)]\delta(8k-b^*) \\
& +\tfrac{3}{4}h\{\eta_4(k)\eta_4^2(3k)\cos[\epsilon_4(k)+2\epsilon_4(3k)]+\eta_1^2(2k)\eta_4(3k)\cos[2\epsilon_1(2k)+\epsilon_4(3k)]\}\delta(7k-b^*) \\
& +\tfrac{1}{4}h\eta_4^3(3k)\cos[3\epsilon_4(3k)]\delta(9k-b^*)+\tfrac{3}{4}h\eta_4^2(k)\eta_1(2k)\cos[2\epsilon_4(k)-\epsilon_1(2k)] \\
& +C_{4444}(0,0,0,0)\eta_4^4(0)+3C_{4444}(0,0,k,-k)\eta_4^2(0)\eta_4^2(k)+3C_{4444}(0,0,3k,-3k)\eta_4^2(0)\eta_4^2(3k) \\
& +3C_{4444}(0,k,k,-2k)\eta_4(0)\eta_4^2(k)\eta_4(2k)\cos[\epsilon_4(0)]\cos[2\epsilon_4(k)-\epsilon_4(2k)] \\
& +\tfrac{3}{8}C_{4444}(k,k,-k,-k)\eta_4^4(k)+\tfrac{3}{2}C_{4411}(k,-k,2k,-2k)\eta_4^2(k)\eta_1^2(2k)+\cdots . \qquad \text{(A1)}
\end{aligned}
$$

The majority of terms of the expansion (A1) are normal. These terms occur for any values of the wave vectors k. Some umklapp terms appear only when the wave vector takes the commensurate values $k=b^*/7$, $b^*/8$, $b^*/9$. Then the umklapp terms give additional contributions to the free energy and usually produce a stable superstructure.

*Present address: Institute of Nuclear Physics, ul. Radzikowskiego, PL-31-342, Krakow, Poland.

[1] M. Elcombe and J. C. Taylor, Acta Crystallogr. Sect. A 24, 410 (1968).

[2] A. L. Solomon, Phys. Rev. 104, 1191 (1956).

[3] H. Futama, Y. Shiozaki, A. Chiba, E. Tanaka, T. Mitsui, and J. Furuichi, Phys. Lett. 25A, 8 (1967).

[4] A. H. Moudden, F. Denoyer, and M. Lambert, J. Phys. (Paris) 39, 1323 (1978).

[5] A. H. Moudden, F. Denoyer, M. Lambert, and W. Fitzgerald, Solid State Commun. 32, 933 (1979).

[6] F. Denoyer, A. H. Moudden, A. Bellamy, R. Currat, C. Vettier, and M. Lambert, Phys. Rev. B 25, 1697 (1982).

[7] E. F. Westrum and J. P. McCullough, in *Physics and Chemistry of the Organic Solid State,* edited by D. Fox, M. M. Labes, and A. Weissberger (Interscience, New York, 1963), Vol. 1.

[8] J. P. Benoit and J. P. Chapelle, Solid State Commun. 4, 883 (1974).

[9] B. Jakubowski and J. W. Rohleder, Mol. Cryst. Liq. Cryst. 46, 157 (1978).

[10] G. J. Goldsmith and J. G. White, J. Chem. Phys. 31, 1175 (1959).

[11] J. Klimowski, W. Wanarski, and D. Ozgo, Phys. Status Solidi A 34, 697 (1976).

[12] M. R. Truter, Acta Crystallogr. Sect. A 22, 556 (1967).

[13] Y. Shiozaki, Ferroelectrics 2, 245 (1971).

[14] D. R. MacKenzie, J. Phys. C 8, 1607 (1975).

[15] F. Denoyer, A. H. Moudden, and M. Lambert, Ferroelectrics 24, 43 (1980).

[16] D. R. MacKenzie, J. Phys. C 8, 2003 (1975).

[17] O. V. Kovalev, *Irreducible Representations of the Space Groups* (Gordon and Breach, New York, 1965).

[18] S. Aubry, in *Seminar on the Riemann Problem, Spectral Theory and Complete Integrability,* Vol. 925 of *Lecture Notes in Mathematics,* edited by D. G. Chudnovsky (Springer, New York, 1980).

[19] F. Axel and S. Aubry, J. Phys. C 14, 5433 (1981).

[20] A. P. Levanyuk and D. G. Sannikov, Fiz. Tverd. Tela 18, 1927 (1976) [Sov. Phys.—Solid State 18, 1122 (1976)].

[21] Y. Ishibashi and Y. Takagi, J. Phys. Soc. Jpn. 46, 143 (1974).

[22] P. Lederer and C. M. Chaves, J. Phys. (Paris) Lett. 42, L127 (1981).

[23] K. Yoshimitsu and T. Matsubara, Suppl. Prog. Theor. Phys. 63, 465 (1980).

[24] T. Janssen and J. A. Tjon, Phys. Rev. B 25, 3767 (1982); 24, 2245 (1981).

[25] A. H. Moudden, Ph.D. thesis, University of Paris, Orsay, 1980 (unpublished).

[26]W. L. McMillan, Phys. Rev. B 14, 1496 (1976).
[27]P. Bak and V. J. Emery, Phys. Rev. Lett. 36, 978 (1976).
[28]I. E. Dzyaloshinskii, Zh. Eksp. Teor. Fiz. 47, 992 (1964) [Sov. Phys.—JETP 20, 665 (1965)].
[29]J. D. Axe, Oak Ridge Laboratory Report No. CONF-760601-PI353, 1976 (unpublished).
[30]A. D. Bruce and R. A. Cowley, J. Phys. C 11, 3609 (1978).
[31]K. Parlinski, following paper, Phys. Rev. B 28, 410 (1983).
[32]M. E. Fisher and W. Selke, Philos. Trans. R. Soc. London 302, 1 (1981).
[33]P. Bak, in *Recent Developments in Condensed Matter Physics*, edited by J. Devreese, V. Van Doren, and L. Lemmens (Plenum, New York, 1981), Vol. 1, p. 489.
[34]D. E. Moncton, J. D. Axe, and F. J. DiSalvo, Phys. Rev. Lett. 34, 734 (1975).
[35]M. Iizumi, J. D. Axe, G. Shirane, and K. Shimaoka, Phys. Rev. B 15, 4392 (1977).
[36]K. Parlinski and K. H. Michel (unpublished).